Acylgermanes: Photoinitiators and Sources for Ge-Centered Radicals. Insights into their Reactivity

Dmytro Neshchadin,[†] Arnulf Rosspeintner,[‡] Markus Griesser,[†] Bernhard Lang,[‡] Sandra Mosquera-Vazquez,[‡] Eric Vauthey,[‡] Vitaly Gorelik,[†,#] Robert Liska,[∥,∇] Christian Hametner,[∥] Beate Ganster,[∥] Robert Saf,[§] Norbert Moszner,[⊥] and Georg Gescheidt*,[†]

[†]Institute of Physical and Theoretical Chemistry and [§]Institute of Chemistry and Technology of Materials, Graz University of Technology, Stremayrgasse 9, 8010 Graz, Austria

[‡]Département de Chimie Physique, Université de Genève, 30, quai Ernest-Ansermet, 1211 Genève 4, Switzerland

[∥]Institute of Applied Synthetic Chemistry, Vienna University of Technology, Getreidemarkt 9/163/MC, 1060 Vienna, Austria

[⊥]Ivoclar Vivadent AG, Bendererstrasse 2, 9494 Schaan, Liechtenstein

[∇]Christian Doppler Laboratory for Photopolymers in Digital and Restorative Dentistry, Getreidemarkt 9, 1060 Vienna, Austria

S *Supporting Information*
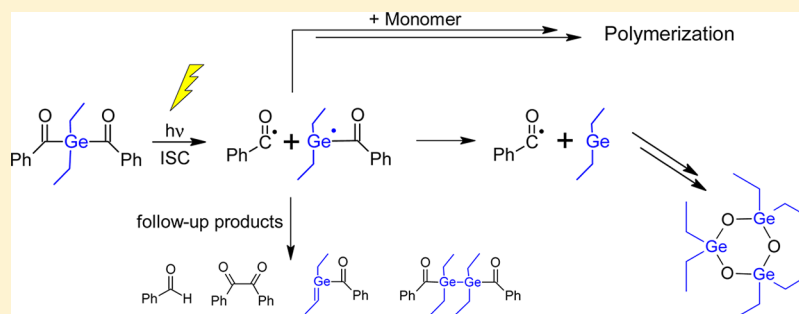
ABSTRACT: Acylgermanes have been shown to act as efficient photoinitiators. In this investigation we show how dibenzoyldiethylgermane **1** reacts upon photoexcitation. Our real-time investigation utilizes femto- and nanosecond transient absorption, time-resolved EPR (50 ns), photo-chemically induced dynamic nuclear polarization, DFT calculations, and GC-MS analysis. The benzoyldiethylgermyl radical G• is formed via the triplet state of parent **1**. On the nanosecond time scale this radical can recombine or undergo hydrogen-transfer reactions. Radical G• reacts with butyl acrylate at a rate of $1.2 \pm 0.1 \times 10^8$ and $3.2 \pm 0.2 \times 10^8$ M^{-1} s^{-1}, in toluene and acetonitrile, respectively. This is ~1 order of magnitude faster than related phosphorus-based radicals. The initial germyl and benzoyl radicals undergo follow-up reactions leading to oligomers comprising Ge−O bonds. LC-NMR analysis of photocured mixtures containing **1** and the sterically hindered acrylate 3,3-dimethyl-2-methylenebutanoate reveals that the products formed in the course of a polymerization are consistent with the intermediates established at short time scales.

1. INTRODUCTION

Germanium-centered radicals are key intermediates in a broad range of chemical reactions.[1−7] The reactivity of the related tin- and silicon-based radicals has been well described, but the reactivity of the related Ge-centered radicals is much less explored.[8−13]

In the field of photoinitiated free-radical polymerization[14,15] Ge-centered radicals have started to play an important role. Especially for applications requiring longer excitation wavelengths (e.g., dental fillings), optimizations of photoinitiators are highly desirable. The recently developed dibenzoyldiethylgermane **1**[16,17] shows the absorption maximum of its n−π* transition, which is required for α-cleavage reactions leading to radicals, at red-shifted 418 nm. The overlap of the d-orbitals of Ge with the π* orbital of the carbonyl group is responsible for that shift. In classical hydroxyalkylphenones this transition can

be found at ~350 nm. Up to now the highest shift for type I photoinitiators was observed for bis-acylphosphine oxides with shifts <400 nm.
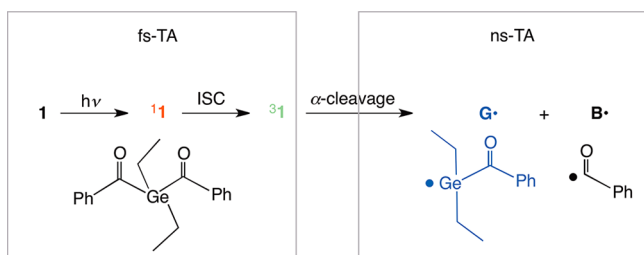

1
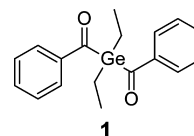
The efficiency of **1** has been demonstrated,[16−19] in terms of photo-DSC measurements and product analysis. However, the primary species leading to the polymerization process have not been established by experiment. As shown in Scheme 1, the

Scheme 1. Reaction Scheme of the Relevant Photophysical Processes of 1 upon Laser Excitation[a]

[a]The grey boxes refer to the processes observable with the respective experimental techniques. The colors of the species correspond to those in the transient absorption spectra (Figure 1).

primary reaction expected is the α-cleavage of a Ge–C(O) bond. Whereas the reactivity of the benzoyl radical is rather well established,[20–23] the knowledge on the Ge-centered radicals requires some expansion.[10]

The aim of our work is to establish the mechanism of the primary cleavage of **1** and to investigate the properties of the thus formed Ge-centered radical. This germyl radical will be described in terms of its structure and its intrinsic conversions; furthermore its reactivity toward acrylate double bonds will be explored quantitatively. This is accomplished by time-resolved optical spectroscopy (fs–μs), time-resolved electron paramagnetic resonance (TR-EPR) (ns), photo-chemically induced dynamic nuclear polarization (CIDNP), EI-MS, and DFT calculations. In addition to the primary reactions of the germyl radical, we show conversions of **1** at long-term irradiation (up to 600 s) in the presence of butyl acrylate and the sterically hindered acrylate 3,3-dimethyl-2-methylenebutanoate (to avoid formation of insoluble polymers). We predominately focus on the chemistry of the Ge-centered radicals, showing some general features of their characteristic transformations.

2. EXPERIMENTAL SECTION

The synthesis of **1** is described in refs 16 and 17. Toluene, toluene-d_8 (Fluka), and acetonitrile-d_3 were used as received. Samples were saturated with Argon prior to use to remove the oxygen from the solution.

For time-resolved optical spectroscopy, toluene (Fisher Scientific, >99.8%), acetonitrile (Fisher Scientific, 99.98%), and butylacrylate (Sigma-Aldrich) were used as received.

The apparatus used for femtosecond transient absorption (fs-TA) spectra with excitation at 400 nm was already described.[24] The instrument response function had a full width at half-maximum (fwhm) of ~200–500 fs as obtained from measurements of the optical Kerr effect in toluene and acetonitrile. Samples were excited with ~10^{15} photons/(cm^2 pulse). Samples were bubbled with nitrogen during the experiment to constantly refresh the excitation volume, thus avoiding sample decomposition. Changes in the sample concentration due to degradation and/or solvent evaporation were negligible as judged from absorption spectra before and after the experiments.

Nanosecond transient absorption (ns-TA) experiments were performed with excitation at 355 nm using a setup described in ref 25. Samples were saturated with nitrogen and constantly bubbled with nitrogen to refresh the sample and avoid sample decomposition.

Rate constants were extracted from the experimental spectra by global target analysis.[26]

TR-EPR experiments were performed using light pulses (355 nm, ~10 mJ/pulse, pulse length ~10 ns) from a Continuum Surelight II Nd:YAG laser, operating at 20 Hz. A Bruker ESP 300E X-band spectrometer with unmodulated static magnetic field and a LeCroy 9400 dual 125 MHz digital oscilloscope were used to acquire the TR-

EPR spectra. During a TR-EPR experiment the desired magnetic field range was scanned by recording the accumulated (50–100 accumulations) EPR time responses to the incident laser pulses at a given static magnetic field. The experimental setup was controlled using fsc2, software developed and kindly provided by J. Toerring (Berlin). Argon-saturated solutions were irreversibly pumped through a quartz tube (inner diameter 2 mm, flow ~2–3 mL/min) in the rectangular cavity of the EPR spectrometer.

^{1}H NMR and CIDNP experiments were carried out on a 200 MHz Bruker AVANCE DPX spectrometer equipped with a custom-made CIDNP probe head. A Spectra Physics INDI Nd:YAG laser (355 nm, ~60 mJ/pulse, pulse length ~8–10 ns) operating at 20 Hz and a Hamamatsu Hg–Xe lamp (150 W, pulse length 300 ms) served as light sources. The typical CIDNP timing sequence consists of the following parts: composite pulse presaturation, laser/lamp flash, 90° radiofrequency detection pulse (2.2 μs), and FID. Sample decomposition during the CIDNP experiment did not exceed 1%, as controlled by NMR.

Geometry optimizations, hyperfine coupling constant (hfc) calculations and frequency analysis were done using the Gaussian 03[27] software package at the B3LYP[28,29] level of theory with the TZVP[30] basis set. Single point energy calculations were carried out using the M052X/6-311+G(2d,2p) protocol.[31]

GC-TOF MS analyses of irradiated solutions of **1** in CD$_3$CN (c = 4.8 × 10^{-6} mol/L, irradiation time up to 2 min, under Ar) were performed on an Agilent 7890A (Agilent, USA) gas chromatograph coupled to an orthogonal TOF mass spectrometer (GCT Premier, Waters). The GC conditions were as follows: column, DB-5MS (J & W Scientific, CA, USA) 30 m length × 0.25 mm ID × 0.25 μm phase thickness; injection temperature, 250 °C; transfer line temperature, 250 °C; column temperature program, 40 °C for 4 min, ramp at 20 °C/min to 280 °C, with a final 4 min hold at 280 °C; carrier gas, helium 1.00 mL/min; injection mode, split 1:100; and injection volume, 1 μL. Mass spectra were acquired in electron ionization mode (70 eV, source temperature 250 °C), over the mass range m/z 50–800 Da, with ~7000 fwhm resolution and an acquisition rate of 4 spectra/s. Data were processed using MassLynx (version 4.1) software.

Photolysis experiments in the presence of the monomer 3,3-dimethyl-2-methylenebutanoate (**t-BAM**)[32] were performed with a Bluephase C8 long-term irradiation (LED) lamp (430–530 nm). The corresponding LC-NMR spectra were recorded on a 400 MHz Bruker Avance DRX400 FT-NMR spectrometer with a 60 μL triple-resonance flow probe head. LC was carried out on an Agilent 1100 HPLC with quaternary pump, UV detector, and solid-phase extraction unit SEP Prospekt 2.

3. RESULTS AND DISCUSSION

3.1. Photophysics. Time-resolved optical spectroscopy was used to obtain information how and on which time scale a Ge-centered radical is formed. We performed femto- and nanosecond broadband transient absorption experiments. Directly after photoexcitation we observe a transient absorption spectrum with a maximum around 470 nm, which we can attribute to the singlet excited state of **1**. This species disappears within tens of picoseconds (cf. Table 1) to give rise to the triplet state of **1**, which exhibits absorption maxima at 460 nm and above 700 nm (green line, upper part of Figure 1).

On the nanosecond time scale, it can be observed that the triplet state of **1** decays within ~15 ns and a new band at 500

Table 1. Rate Constants of Inter System Crossing (ISC) and α-Cleavage of 1

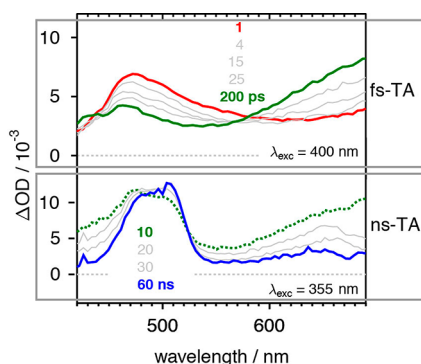| solvent	k_{ISC}, s^{-1}	k_{cleav}, s^{-1}
toluene	$(3 \pm 0.3)\cdot10^{10}$	$(6 \pm 2)\cdot10^{7}$
acetonitrile	$(2 \pm 0.1)\cdot10^{10}$	$(7 \pm 2)\cdot10^{7}$

Figure 1. Femto- and nanosecond transient absorption spectra of **1** in toluene. The upper part shows the time regime between 1 and 200 ps, whereas the lower part represents the nanosecond experiment 10−60 ns (see Experimental Section). Note, that the dashed green spectrum in the lower part corresponds to a spectrum comprising ^{3}**1** and **G●**.

nm emerges (Figure 1, lower part). This absorption can straightforwardly be ascribed to the Ge-centered radical **G●** since the simultaneously formed benzoyl radical **B●** is known not to be detectable in the 400−700 nm range.[21]

Accordingly, the reaction sequence sketched in Scheme 1 can be adopted. Whereas the rate constant for inter system crossing has an expectable value of $\sim 3 \times 10^{10}$ s^{-1}, the rate constant for α-bond cleavage is relatively small ($\sim 7 \times 10^7$ s^{-1}). This is in remarkable contrast to the photophysics of the P containing analog, the intersystem crossing rate of which is reported to be 8×10^9 s^{-1} and its cleavage rate being much faster with 10^{10} s^{-1}.[21] The corresponding rate constants are summarized in Table 1.

3.2. TR-EPR. With a time resolution of ~ 50 ns, and its rather high sensitivity based on radical-pair effects,[33−36] TR-EPR is ideally suited to get insight into the structure of the primary Ge-centered radical **G●**. Laser-flash photolysis of **1** leads to the TR-EPR spectrum shown in Figure 2. It consists of two
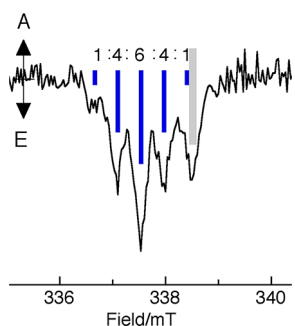

Figure 2. TR-EPR spectrum of **1** in toluene, taken 250 ns after the laser flash, showing two different EPR signals: **G●** (blue) and **B●** (gray).

different overlapping signals appearing in emission, indicating that radicals are polarized via the triplet mechanism,[34,37] in line with the results obtained by optical spectroscopy. The rather narrow and unresolved signal ($g = 2.000$, marked in gray in Figure 2) is attributed to the benzoyl radical **B●**.[20,38] The dominating pattern ($g = 2.006$, blue in Figure 2) is a quintet (intensity ratio 1:4:6:4:1), with an isotropic ^{1}H hfc of 0.44 mT. It can be assigned readily to the four equivalent methylene protons ("β-hydrogens") of the two ethyl groups in the Ge-centered radical[39] **G●** (calcd ^{1}H hfc, 0.61 mT). Moreover,

calculations show that the remaining ^{1}H hfcs (γ- and aromatic protons) in **G●** are at least 1 order of magnitude smaller and are not resolved in the experimental TR-EPR spectrum (see Supporting Information).[40]

The TR-EPR experiments clearly establish radicals **B●** and **G●** as the primary species formed on a 50 ns time scale upon irradiation of **1** after intersystem crossing from the excited singlet to the excited triplet state and subsequent α-cleavage (Scheme 1).

3.3. ^{1}H TR-CIDNP. When an initiator is photolyzed and undergoes a homolytic bond cleavage, the corresponding radical pair is created in a correlated spin state. The follow-up reactions of this initially formed radicals depend on the relative orientations of their spins, e.g., two radicals with an overall triplet state cannot recombine, causing a non-Boltzmann population of magnetic energy levels (up to a μs time scale) and leading to 'polarized' NMR signals. Therefore, reaction pathways proceeding via radical pairs can preferentially be followed using this phenomenon (CIDNP).[41,42] We have applied the time-resolved ^{1}H CIDNP technique[43−45] to investigate primary transformations of the radicals **G●** and **B●**.

In Figure 3, the ^{1}H NMR spectrum of parent **1** and the corresponding TR-CIDNP resonances with delays of 1 and 20 μs (in toluene-d_8) are presented. The spectra taken 1 and 20 μs after the laser flash show compatible polarization patterns but indicate that additional follow-up products emerge after 20 μs.

The resonances can be assigned in the following way: In the 1 μs TR-CIDNP spectrum (Figure 3B) methylene protons of parent **1** appear in strong enhanced absorption. This can be attributed to the (geminate or cage) reformation of **1** from **G●** and **B●**.[46] Using Kaptein's rule[47−49] for the net polarization and taking into account the g factor and the ^{1}H hfcs of **G●** and **B●** (enhanced absorption, $\Delta g > 0$, hfc(CH$_2$) > 0, derived from EPR and DFT calculations, respectively, see above) it can be deduced that the primary radical pair is created in the triplet excited state, in full agreement with the emissive polarization pattern of the TR-EPR signals (Figure 2) and in line with related photoinitiators.[50]

The initial radicals also diffuse apart and yield 'escape' products. A well-established reaction is the dimerization of two identical radicals leading to **2** (formed from two **G●**, related to the reactivity of phosphinoyl radicals)[51] and diphenylethane-1,2-dione (benzil, **6**, from two **B●**).

The signals assigned to **2** are the emissive resonances at $\delta = 1.31$ and 1.74 ppm, for CH$_3$ and CH$_2$ respectively, in agreement with Kaptein's rule for the net CIDNP polarization. ^{1}H CIDNP resonances of **6** can hardly be distinguished because the small hfcs of phenyl protons of the precursor (benzoyl radical) lead to very weak polarization intensities and the aromatic region contains many overlapping peaks.

Even after the short delay of 1 μs, new resonances appear with distinct polarizations. In particular, a singlet in enhanced absorption at $\delta = 9.59$ ppm and a negatively polarized multiplet at $\delta = 7.54$ ppm emerge. These resonances are typical for the carbonyl and ortho-phenyl protons of benzaldehyde **3** and have been frequently observed for several photoinitiating systems containing the benzoyl moiety.[52] Formation of **3** is usually attributed to a disproportionation reaction (β-hydrogen transfer)[52] in the primary radical pairs consisting of a benzoyl radical and radicals, which are able to donate hydrogen atoms. In the present case, the hydrogen has to be transferred from the ethyl group of **G●** as shown in Scheme 2.
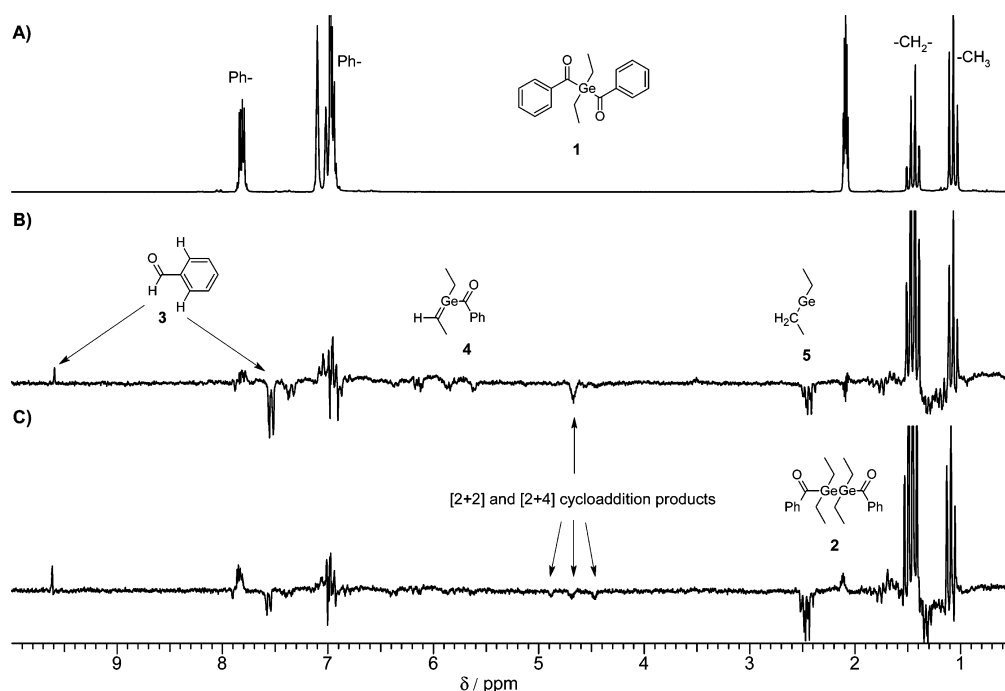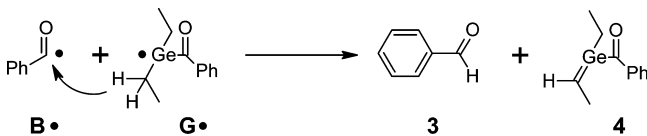
Figure 3. ^{1}H NMR (A), 1 μs (B) and 20 μs (C) TR-CIDNP spectra of **1** in toluene-d_8.

Scheme 2. Possible Hydrogen Transfer Reaction within the Primary Radical Pair (G• and B•) Formed upon Photoinduced α-Cleavage of 1


According to Kaptein's rules, aldehyde **3** is observed on the time scale of our experiment as a cage product (enhanced absorption, triplet precursor, $\Delta g > 0$, hfc(CH$_2$) > 0).

The resonances of vinyl hydrogens at δ = ~5.7 ppm point at *E*- and *Z*-isomers of a (transient) germene **4** (Scheme 2).

The strongly emissive quartet at δ = 2.44 ppm (J = 7.1 Hz) can be provisionally assigned to the methylene protons of diethylgermylene **5** (Figure 3B) as the result of a second cleavage at the stage of **G•** leading to **5** and a second benzoyl radical **B•** (Scheme 3). This assignment is provisional since we neither found ^{1}H NMR spectroscopic information for Ge(II) nor for similar Si(II) and Sn(II) species. The decomposition of **G•** is feasible according to M052X/6-311+G(2d,2p) DFT

Scheme 3. Cleavage of Ge-Centered Radical G•
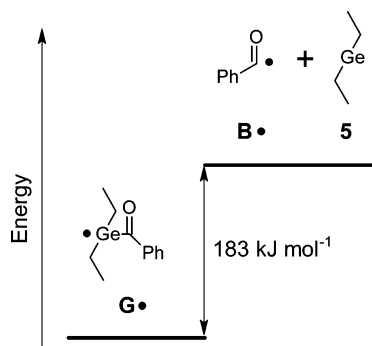
calculations, which predict the bond dissociation energy of the Ge−C bond in **G•** being only 183 kJ mol^{-1}. Since Ge(II)-containing species are known to be highly reactive without additional stabilization (e.g., by donor−acceptor substitution),[53−55] **5** is rapidly converted to more persistent products (see Section 3.4) and cannot be established after longer reaction periods.

In the CIDNP spectrum taken 1 μs after the laser flash, two weaker emissive signals are observed at δ = 4.67 and 4.81 ppm. These signals presumably do not stem directly from the initial radicals **G•** and **B•**. These resonances might be due to secondary products generated via rapid follow-up reactions of an intermediate germene **4**.

Germenes are reported to undergo fast and almost quantitative [2 + 2] and [2 + 4] cycloadditions[56−59] in the presence of saturated and unsaturated ketones, respectively. The thus formed heterocycles are likely to undergo further transformations. Accordingly, the signals at δ = 4.67 and 4.81 ppm, the emissively polarized signals at ca. δ = 6.15 ppm and two multiplets (δ = 4.47 and 4.88 ppm) in the 1 and 20 μs TR-CIDNP spectra (Figure 3B,C) could originate from such products. Scheme 4 summarizes the short-lived intermediates (up to 20 μs), which have been established (and, partly, anticipated) from TR-EPR and ^{1}H TR-CIDNP experiments.

3.4. GC-MS Analysis of "Relaxed" Reaction Mixtures. The above experiments have shown reaction products obtained upon laser-flash photolysis (355 nm, 10 ns pulse) up to a microsecond time scale, creating the basis for conversions, following at longer irradiation times. In technical applications, however, irradiation is performed over a period in the order of seconds. To obtain insight into products formed at extended time scales and under thermodynamic control, GC-TOF MS analysis of reaction solutions treated with different periods of irradiation was performed.

Generally, follow-up products compatible with the formation of benzoyl radical **B•** could be well established, e.g., benzaldehyde **3** and benzil **6** were found as the main products.

Scheme 4. Reaction Pattern of the Primary Radicals B• and G•
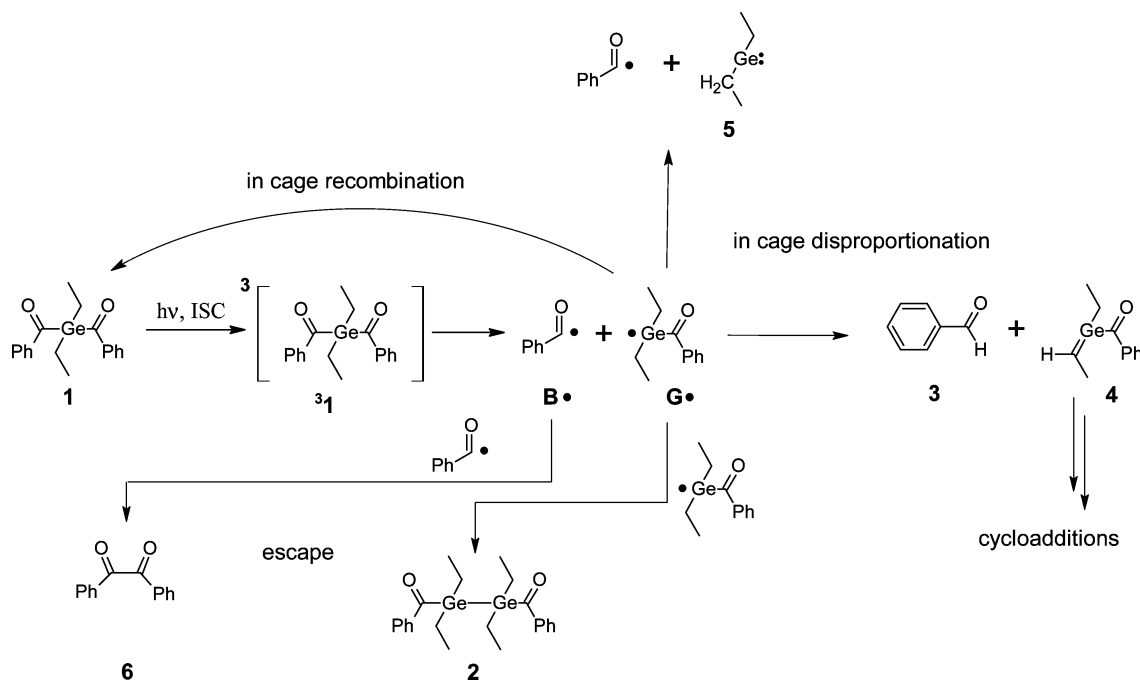
Additionally, small amounts of phenol and benzoic acid were detected. In the case of products formed via Ge-centered radical G•, where ^{1}H CIDNP and ^{1}H NMR only provided early products, mass spectra were observed, that can be assigned to products revealing Ge−O bonds, especially cyclic products $(GeEt_2O)_n$ (7_n).
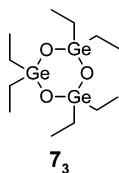
As an example, the most important product containing germanium was detected at a retention time t_R = 12.7 min and is assigned to 7_3. The base peak in the corresponding mass spectrum was observed at m/z = 410.9473 Da, which corresponds well to the calculated mass of the fragment ion $[7_3\text{-Et}]^+$ ($C_{10}H_{25}Ge_3O_3$; m/z_{calc} = 410.9469 Da). The molecular ion 7_3^+ was observed too, but only with very low relative intensity and consequently low mass accuracy. The homologous products 7_n with n = 4 and 5 were observed at t_R = 14.6 and 16.4 min, respectively. Furthermore, other volatile products were detected at low concentration, where the fragmentation pattern as well as the accurate mass data indicated species like $(GeEt_{2n-1}O)_nBz$ (Bz = benzoyl-), e.g., $(GeEt_{2n-1}O)_4Bz$ at a retention time of t_R = 17.9 min.

The formerly suggested oligomeric Ge−Ge bonded species,[19] anticipated from broadened ^{1}H NMR lines, could not be discerned. This is not astonishing in view of the relatively weak Ge−Ge bond (~270 kJ mol^{-1}) compared to, e.g., a Ge−O bond (662 kJ mol^{-1}), which is certainly more likely to be formed under these reaction conditions favoring thermodynamic control. The results discussed above imply that oligomeric and probably also polymeric (cyclic) molecules with O−Ge−O connectivity are formed.

3.5. Addition of Radical G• to Double Bonds.

It has been shown that the acylgermane photoinitiator **1** is rather efficient from a technical point of view.[16−18] Obviously, both radicals G• and B• add to (acrylate) double bonds. The kinetic data for B• were determined by time-resolved IR spectroscopy.[21]

We have measured the rate constant of the addition of G• to butyl acrylate using ns-TA spectroscopy, by following the decay of the absorption at ~500 nm (cf. Figure 1). The plots showing the dependence of the observed (pseudo first order) rate constant vs the concentration of butyl acrylate are shown in Figure 4.
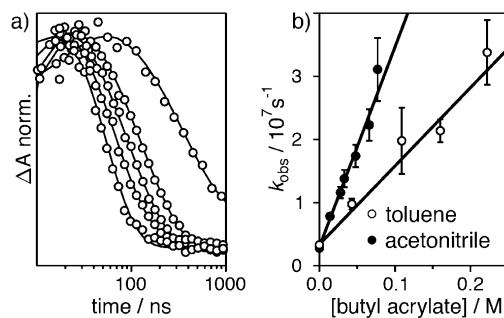

Figure 4. (a) Decay curves obtained from ns-TA experiments at different butyl acrylate concentrations (0, 0.014, 0.028, 0.048, 0.077 M; observation wavelength, 507 nm; solvent, acetonitrile); (b) pseudofirst-order decay rate constants, k_{obs}, obtained from (a) as a function of butyl acrylate concentration in toluene and acetonitrile for the determination of k_{add}.

The corresponding addition rate constants, k_{add}, are 1.2×10^8 and 3.2×10^8 M^{-1} s^{-1}, in toluene and acetonitrile, respectively, are compatible with those determined for the triphenylgermyl radical **PhG•**[50] (Table 2).

The k_{add} values for the Ge-centered radicals are substantially higher than those of the radical B• (3 orders of magnitude).

Table 2. Experimentally Established Rate Constants for the Addition of the Radicals G• to Butyl Acrylate and PhG• to Methyl Acrylate

radical	solvent	k_{add}, M^{-1} s^{-1}	ref
G•	toluene	$(1.2 \pm 0.1) \times 10^8$	this work
G•	acetonitrile	$(3.2 \pm 0.2) \times 10^8$	this work
PhG•	acetonitrile	2.2×10^{8a}	50
B•	acetonitrile	2.7×10^5 ($\pm 10\%$)	21

[a]No error limits given.

Thus, the **G•** is the prominently active radical generated from photoinitiator **1**. It is moreover, noteworthy, that the substituents do not markedly alter the rate constants for the addition of the Ge center to double bonds.

3.6. Photolysis in the Presence of 3,3-dimethyl-2-methylenebutanoate (*t*-BAM). For the application of photoinitiator **1** in polymerizations, usually LEDs and longer irradiation times are applied. To investigate if the species established by the time-resolved experiments at very short time scales described above also are decisive during a polymerization, photolysis experiments (LED lamp, 430−530 nm) of **1** in the presence of *t*-BAM (6 equiv) were performed in acetonitrile. The products were analyzed by LC-NMR.

The LC presents nine prominent components (Figure 7, individual NMR spectra see Supporting Information). These can be clearly assigned to photoproducts of the primary radicals **G•** and **B•**. Benzaldehyde **3** has been identified as a product being formed at very early stages of the decomposition of **1**, based on **B•**. It has, however, to be borne in mind that **3** can also be formed by a partly reversible polymerization process.[60]

When the benzoyl radical reacts with *t*-BAM, the saturated derivative **B1** and the two unsaturated isomers **B2** and **B3** are formed connected with hydrogen transfer. The occurrence of **B4**, where an additional benzoyl moiety is attached to **B1** indicates that benzoyl radicals are even present during the initial steps of the polymerization and are able to add to the growing polymer chain. Interestingly, **2**, the dimer of the benzoyldiethylgermyl radical **G•**, also established by the CIDNP technique still can be detected by LC-NMR. In

analogy to the **B•**-derived molecules **B1** and **B2/3**, products **G1** and **G2** represent the addition of *t*-BAM to **G•**. Whereas the saturated product **B1** dominates in the case of **B•** as the precursor, unsaturated **G2** shows a higher LC peak intensity. Owing to the characteristics of the LED utilized, further photochemical decomposition of **G1** and **G2** is not observed. In irradiation experiments at 365 nm, these products occurred only in traces because immediate photochemical decomposition occurred at shorter-wavelength irradiation. Another remarkable product is **GMB**. It can be either based on a **B**-(*t*-BAM) radical and addition of **G•** or a **G**-(*t*-BAM) radical reacting with **B•**.

4. CONCLUSION

The germanium based photoinitiator **1** displays a substantial efficiency for initiating radical polymerization. Its red-shifted n−π* absorption provides excellent usability. Parent **1** cleaves upon irradiation to give the radical pair **B•** (benzoyl) and **G•** (germyl). These two radicals are the primary species initiating radical polymerizations.

On short time scales, **G•** radicals can form germylenes (H-transfer) or dimerize, however, the substantial preference of Ge toward oxygen leads to the formation of products displaying (Ge−O)$_n$ moieties.

It is remarkable that long-term irradiation (LED) and short-time scale experiments (laser) reveal rather similar products. This can be traced back to the low energy of the LED utilized for these experiments but is also consistent with a partially reversible addition−elimination mechanism of the parent radicals toward the double bonds followed by hydrogen transfer.[60,61]

Our investigations suggest that the substituents around a Ge radical center should not have a very high impact on the reactivity of the radical toward (acrylate) double bonds. This is in line with published data[50] but certainly needs substantiation. Another important factor will be the investigation of the reactivity of Ge-centered radicals with oxygen.
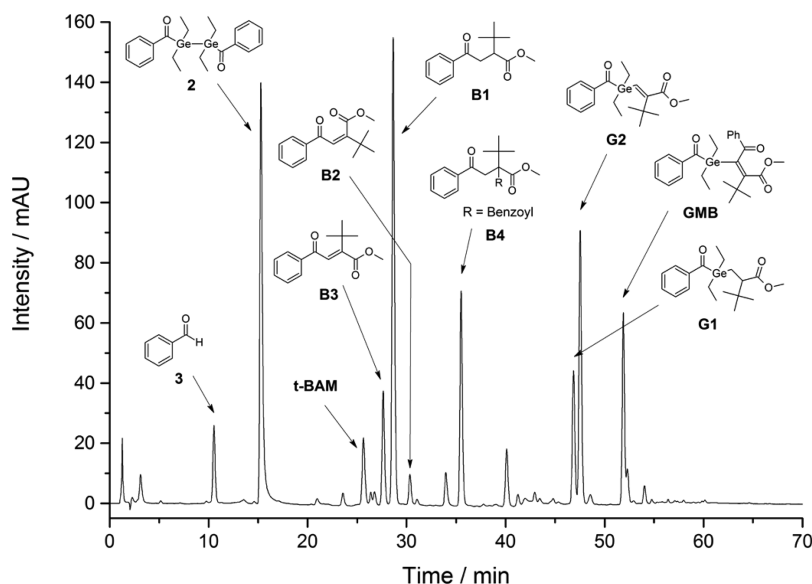

Figure 7. Optimized LC chromatogram for the NMR detection of the photolysis solution of **2** in acetonitrile (detection wavelength 225 nm).

ASSOCIATED CONTENT

Supporting Information

Geometry and calculated hfcs of radicals **B•** and **G•**, LC-NMR spectra. This information is available free of charge via the Internet at http://pubs.acs.org/.

AUTHOR INFORMATION

Corresponding Author

g.gescheidt-demner@tugraz.at

Notes

The authors declare no competing financial interest.
#Deceased.

ACKNOWLEDGMENTS

REFERENCES

(1) Lloyd, R. V.; Rogers, M. T. *J. Am. Chem. Soc.* **1973**, *95*, 2459.

(2) Drost, C.; Griebel, J.; Kirmse, R.; Lonnecke, P.; Reinhold, J. *Angew. Chem., Int. Ed.* **2009**, *48*, 1962.

(3) Herrmann, W. A.; Denk, M.; Behm, J.; Scherer, W.; Klingan, F. R.; Bock, H.; Solouki, B.; Wagner, M. *Angew. Chem.* **1992**, *104*, 1489.

(4) Sheberla, D.; Tumanskii, B.; Tomasik, A. C.; Mitra, A.; Hill, N. J.; West, R.; Apeloig, Y. *Chem. Sci.* **2010**, *1*, 234.

(5) Power, P. P. *Chem. Rev.* **2003**, *103*, 789.

(6) Lee, V. Y.; Sekiguchi, A. In *Reviews of Reactive Intermediate Chemistry*; Platz, M. S., Moss, R. A., Jones, J., M., Eds.; John Wiley & Sons, Inc.: Hoboken, NJ, 2007, pp 47−120.

(7) Lee, V. Y.; Sekiguchi, A. *Organometallic Compounds of Low-Coordinate Si, Ge, Sn and Pb: From Phantom Species to Stable Compounds*; Wiley & Sons Inc.: Chichester, 2010.

(8) Albert, A.; Seconi, G.; Pedulli, G. F.; Degl'innocenti, A. *J. Organomet. Chem.* **1983**, *253*, 291.

(9) Bernardoni, S.; Lucarini, M.; Pedulli, G. F.; Valgimigli, L.; Gevorgyan, V.; Chatgilialoglu, C. *J. Org. Chem.* **1997**, *62*, 8009.

(10) Ingold, K. U.; Lusztyk, J.; Scaiano, J. C. *J. Am. Chem. Soc.* **1984**, *106*, 343.

(11) Krusic, P. J.; Kochi, J. K. *J. Am. Chem. Soc.* **1971**, *93*, 846.

(12) Taraban, M. B.; Volkova, O. S.; Kruppa, A. I.; Leshina, T. V. In *Patai's Chemistry of Functional Groups, Organic Germanium, Tin and Lead Compounds*; Rappoport, Z., Liebman, J. F., Marek, I., Eds.; Wiley: Hoboken, NJ, 2003, p 579.

(13) Wille, U. *Chem. Rev.* **2013**, *113*, 813.

(14) Yagci, Y.; Jockusch, S.; Turro, N. J. *Macromolecules* **2010**, *43*, 6245.

(15) Dietliker, K.; Jung, T.; Benkhoff, J.; Kura, H.; Matsumoto, A.; Oka, H.; Hristova, D.; Gescheidt, G.; Rist, G. *Macromol. Symp.* **2004**, *217*, 77.

(16) Ganster, B.; Fischer, U. K.; Moszner, N.; Liska, R. *Macromolecules* **2008**, *41*, 2394.

(17) Moszner, N.; Fischer, U. K.; Ganster, B.; Liska, R.; Rheinberger, V. *Dent. Mater.* **2008**, *24*, 901.

(18) Moszner, N.; Zeuner, F.; Lamparth, I.; Fischer, U. K. *Macromol. Mater. Eng.* **2009**, *294*, 877.

(19) Durmaz, Y. Y.; Kukut, M.; Moszner, N.; Yagci, Y. *Macromolecules* **2009**, *42*, 2899.

(20) Hristova, D.; Gatlik, I.; Rist, G.; Dietliker, K.; Wolf, J.-P.; Birbaum, J.-L.; Savitsky, A.; Moebius, K.; Gescheidt, G. *Macromolecules* **2005**, *38*, 7714.

(21) Colley, C. S.; Grills, D. C.; Besley, N. A.; Jockusch, S.; Matousek, P.; Parker, A. W.; Towrie, M.; Turro, N. J.; Gill, P. M. W.; George, M. W. *J. Am. Chem. Soc.* **2002**, *124*, 14952.

(22) Dietliker, K.; Broillet, S.; Heltrung, B.; Rzadek, P.; Rist, G.; Wirz, J.; Neshchadin, D.; Gescheidt, G. *Helv. Chim. Acta* **2006**, *89*, 2211.

(23) Voll, D.; Junkers, T.; Barner-Kowollik, C. *Macromolecules* **2011**, *44*, 2542.

(24) Banerji, N.; Duvanel, G.; Perez-Velasco, A.; Maity, S.; Sakai, N.; Matile, S.; Vauthey, E. *J. Phys. Chem. A* **2009**, *113*, 8202.

(25) Lang, B.; Mosquera-Vazquez, S.; Lovy, D.; Sherin, P.; Markovic, V.; Vauthey, E. *Rev. Sci. Instrum.* **2013**, *84*, 73107.

(26) Fita, P.; Luzina, E.; Dziembowska, T.; Radzewicz, C.; Grabowska, A. *J. Chem. Phys. A* **2006**, *125*, 184508.

(27) Frisch, M. J.; Trucks, G. W.; Schlegel, H. B.; Scuseria, G. E.; Robb, M. A.; Cheeseman, J. R.; Montgomery, J. A., Jr.; Vreven, T.; Kudin, K. N.; Burant, J. C.; Millam, J. M.; Iyengar, S. S.; Tomasi, J.; Barone, V.; Mennucci, B.; Cossi, M.; Scalmani, G.; Rega, N.; Petersson, G. A.; Nakatsuji, H.; Hada, M.; Ehara, M.; Toyota, K.; Fukuda, R.; Hasegawa, J.; Ishida, M.; Nakajima, T.; Honda, Y.; Kitao, O.; Nakai, H.; Klene, M.; Li, X.; Knox, J. E.; Hratchian, H. P.; Cross, J. B.; Bakken, V.; Adamo, C.; Jaramillo, J.; Gomperts, R.; Stratmann, R. E.; Yazyev, O.; Austin, A. J.; Cammi, R.; Pomelli, C.; Ochterski, J. W.; Ayala, P. Y.; Morokuma, K.; Voth, G. A.; Salvador, P.; Dannenberg, J. J.; Zakrzewski, V. G.; Dapprich, S.; Daniels, A. D.; Strain, M. C.; Farkas, O.; Malick, D. K.; Rabuck, A. D.; Raghavachari, K.; Foresman, J. B.; Ortiz, J. V.; Cui, Q.; Baboul, A. G.; Clifford, S.; Cioslowski, J.; Stefanov, B. B.; Liu, G.; Liashenko, A.; Piskorz, P.; Komaromi, I.; Martin, R. L.; Fox, D. J.; Keith, T.; Al-Laham, M. A.; Peng, C. Y.; Nanayakkara, A.; Challacombe, M.; Gill, P. M. W.; Johnson, B.; Chen, W.; Wong, M. W.; Gonzalez, C.; Pople, J. A. *Gaussian 03*, revision E.01; Gaussian, Inc.: Wallingford, CT, 2004.

(28) Becke, A. D. *J. Chem. Phys.* **1993**, *98*, 5648.

(29) Stephens, P. J.; Devlin, F. J.; Chabalowski, C. F.; Frisch, M. J. *J. Phys. Chem.* **1994**, *98*, 11623.

(30) Schafer, A.; Huber, C.; Ahlrichs, R. *J. Chem. Phys.* **1994**, *100*, 5829.

(31) Zhao, Y.; Schultz, N. E.; Truhlar, D. G. *J. Chem. Theory Comput.* **2006**, *2*, 364.

(32) Seidl, B.; Liska, R. *Macromol. Chem. Phys.* **2007**, *208*, 44.

(33) *Chemically induced magnetic polarisation*; Muus, L. T.; Atkins, P. W.; McLauchlan, K. A.; Pedersen, J. B., Eds.; D. Reidel: Dordrecht, 1977.

(34) Nagakura, S.; Hayashi, H.; Azumi, T. *Dynamic Spin Chemistry*; Kodansha and John Wiley&Sons co-publication: Tokyo and New York, 1998.

(35) Rodgers, C. T. *Pure Appl. Chem.* **2009**, *81*, 19.

(36) Yurkovskaya, A.; Morozova, O.; Gescheidt, G. In *Encyclopedia of Radicals in Chemistry, Biology and Materials*; Chattilialoglu, C., Studer, A., Eds.; Wiley: Hoboken, NJ, **2012**; Vol. *1*, p 175.

(37) Adrian, F. J. *Res. Chem. Intermed.* **1991**, *16*, 99.

(38) Williams, R. M.; Khudyakov, I. V.; Purvis, M. B.; Overton, B. J.; Turro, N. J. *J. Phys. Chem. B* **2000**, *104*, 10437.

(39) Sakurai, H.; Mochida, K.; Kira, M. *J. Am. Chem. Soc.* **1975**, *97*, 929.

(40) Gerson, F.; Huber, W. *Electron Spin Resonance Spectroscopy of Organic Radicals*; Wiley-VCH: Weinheim, 2003.

(41) Bargon, J.; Fischer, H.; Johnsen, U. *Z. Naturforsch., A: Phys. Sci.* **1967**, *22*, 1551.

(42) Ward, H. R.; Lawler, R. G. *J. Am. Chem. Soc.* **1967**, *89*, 5518.

(43) Closs, G. L.; Miller, R. J. *J. Am. Chem. Soc.* **1979**, *101*, 1639.

(44) Miller, R. J.; Closs, G. L. *Rev. Sci. Instrum.* **1981**, *52*, 1876.

(45) Schaublin, S.; Wokaun, A.; Ernst, R. R. *Chem. Phys.* **1976**, *14*, 285.

(46) Taraban, M. B.; Maryasova, V. I.; Leshina, T. V.; Rybin, L. I.; Gendin, D. V.; Vyazankin, N. S. *J. Organomet. Chem.* **1987**, *326*, 347.

(47) Kaptein, R. *Chem. Commun.* **1971**, 732.

(48) Closs, G. L.; Trifunac, A. D. *J. Am. Chem. Soc.* **1969**, *91*, 4554.

(49) Kaptein, R.; Oosterhoff, L. J. *Chem. Phys. Lett.* **1969**, *4*, 214.

(50) Lalevee, J.; Allonas, X.; Fouassier, J. P. *Chem. Phys. Lett.* **2009**, *469*, 298.

(51) Kolczak, U.; Rist, G.; Dietliker, K.; Wirz, J. *J. Am. Chem. Soc.* **1996**, *118*, 6477.

(52) Borer, A.; Kirchmayr, R.; Rist, G. *Helv. Chim. Acta* **1978**, *61*, 305.

(53) Becerra, R.; Boganov, S. E.; Egorov, M. P.; Lee, V. Y.; Nefedov, O. M.; Walsh, R. *Chem. Phys. Lett.* **1996**, *250*, 111.

(54) Smith, G. R.; Guillory, W. A. *J. Chem. Phys.* **1972**, *56*, 1423.

(55) Thimer, K. C.; Al-Rafia, S. M. I.; Ferguson, M. J.; McDonald, R.; Rivard, E. *Chem. Commun.* **2009**, 7119.

(56) Barrau, J.; Escudie, J.; Satge, J. *Chem. Rev.* **1990**, *90*, 283.

(57) El Kettani, S. E. C.; Lazraq, M.; Ranaivonjatovo, H.; Escudie, J.; Gornitzka, H.; Ouhsaine, F. *Organometallics* **2007**, *26*, 3729.

(58) El Kettani, S. E. C.; Lazraq, M.; Ranaivonjatovo, H.; Escudie, J.; Couret, C.; Gornitzka, H.; Atmani, A. *Organometallics* **2005**, *24*, 5364.

(59) Lazraq, M.; Escudie, J.; Couret, C.; Satge, J.; Soufiaoui, M. *Organometallics* **1992**, *11*, 555.

(60) Griesser, M.; Neshchadin, D.; Dietliker, K.; Moszner, N.; Liska, R.; Gescheidt, G. *Angew. Chem., Int. Ed.* **2009**, *48*, 9359.

(61) Voll, D.; Neshchadin, D.; Hiltebrandt, K.; Gescheidt, G.; Barner-Kowollik, C. *Macromolecules* **2012**, *45*, 5850.